Scaling analysis of unsteady natural convection boundary layer for instantaneous heating

Suvash C. Saha[1*], Feng Xu[2], Md. Mamun Molla[3], Tomasz P. Bednarz[4]

[1]School of Engineering and Physical Sciences, James Cook University, Townsville, QLD 4811, Australia.
[2]School of Civil Engineering, The University of Sydney, NSW 2006, Australia.
[3]Department of Mechanical and Manufacturing Engineering, University of Manitoba, Winnipeg, R3T 5V6, Canada.
[4]CSIRO Earth Science and Resource Engineering, 1 Technology Court, Pullenvale QLD 4069, Australia.

*E-mail of presenting author: s_c_saha@yahoo.com

Abstract Natural convection thermal boundary layer adjacent to an instantaneous heated inclined flat plate is investigated through a scaling analysis and verified by direct numerical simulations. It is revealed from the analysis that the development of the boundary layer may be characterized by three distinct stages, i.e. a start-up stage, a transitional stage and a steady state stage. These three stages can be clearly identified from the numerical simulations. Major scales including the flow velocity, flow development time, and the thermal and viscous boundary layer thicknesses are established to quantify the flow development at different stages and over a wide range of flow parameters. Details of the scaling analysis are described in this paper.

Keywords Instantaneous heating, scaling; boundary layer; Inclined flat plate, .

1. Introduction

Natural convection adjacent to a heated or cooled flat plate is a common phenomenon in nature and industry, and thus the corresponding study is of practical significance in fluid mechanics and heat transfer societies. The flow development of a growing boundary layer may be quantified using scaling analysis [1], which is increasingly adopted by the researchers since it is a cost-effective way that can be applied for understanding the physical mechanism of the fluid flow and heat transfer. The results of scale analysis also play an important role in guiding both further experimental and numerical investigations. A detailed scaling analysis of the various stages of the flow development in a differentially heated cavity following sudden heating and cooling on the vertical boundaries has been addressed in [1].

The flow development in the various stages, including the start up of the vertical boundary layer adjacent to the heated sidewall, the development of the intrusion layer under the ceiling of the cavity and finally the approach of the flow in the cavity to a steady state has been characterized [1]. Subsequently, the scaling relations of the thermal boundary layer for various boundary conditions and geometries have been obtained, some of which have been verified through comparisons with numerical simulations over a range of forcing parameters [2-10]. The scaling analysis has also been applied for the flow development in an attic [8, 10, 11] for both heating and cooling roof conditions. The studies by Saha et al. [8, 10] revisit the attic space problem for two different thermal forcing cases: sudden heating and cooling for a wide range of roof slope.

In this study, a new scaling for the development of the boundary layers adjacent to the downward facing inclined heated flat plate is developed. A suddenly imposed temperature on the plate is considered. The Prandtl number in this study is chosen greater than unity. Detailed balances of the important terms of the N-S and energy equations are examined. The scaling relations of the velocity, thermal and viscous layer thickness in the different stages of the boundary layer development are achieved, and the time scale of the transition of the flow to a steady state is also obtained. The numerical results agree well with the scaling results for all parameters considered here.

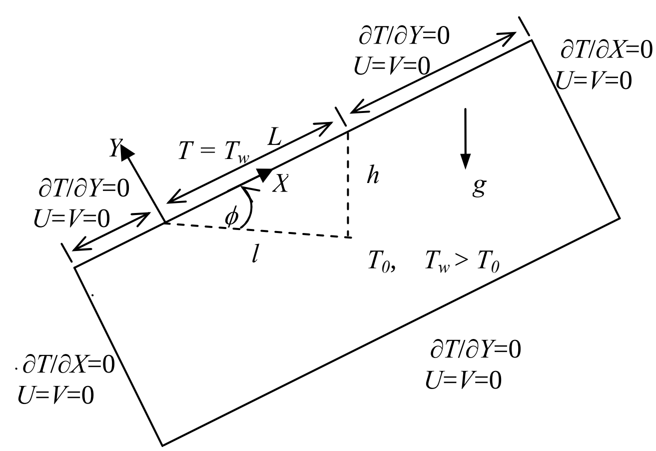

Fig. 1: Schematic of the computational domain and boundary conditions.

2. Problem Formulation

Under consideration is the flow resulting from an initially motionless and isothermal Newtonian fluid (with $Pr > 1$) adjacent to an inclined heated plate. The physical system sketched in Figure 1 consists of an inclined flat plate ($CD = L$). Both ends of the plate are extended by a distance equal to its length and form a rectangular domain, which is filled with an initially stationary fluid at a temperature T_0. If the plate is considered as the hypotenuse of a right angled triangle then the height is h, the length of the base is l and the angle that the plate makes with the base is ϕ. Except for the plate (the section CD shown in Figure 1), all walls of the rectangular domain are assumed to be adiabatic, rigid and non-slip. A sudden heating temperature boundary condition has been applied on the plate which is then maintained.

The development of the flow under the inclined plate is governed by the following two-dimensional Navier–Stokes and energy equation with the Boussinesq approximation:

$$\frac{\partial U}{\partial X}+\frac{\partial V}{\partial Y}=0 \tag{1}$$

$$\frac{\partial U}{\partial t}+U\frac{\partial U}{\partial X}+V\frac{\partial U}{\partial Y} = -\frac{1}{\rho}\frac{\partial P}{\partial X}+\nu\left(\frac{\partial^2 U}{\partial X^2}+\frac{\partial^2 U}{\partial Y^2}\right)+g\sin\phi\beta\left(T-T_0\right) \tag{2}$$

$$\frac{\partial V}{\partial t}+U\frac{\partial V}{\partial X}+V\frac{\partial V}{\partial Y} = -\frac{1}{\rho}\frac{\partial P}{\partial Y}+\nu\left(\frac{\partial^2 V}{\partial X^2}+\frac{\partial^2 V}{\partial Y^2}\right)+g\cos\phi\beta\left(T-T_0\right) \tag{3}$$

$$\frac{\partial T}{\partial t}+U\frac{\partial T}{\partial X}+V\frac{\partial T}{\partial Y}=\kappa\left(\frac{\partial^2 T}{\partial X^2}+\frac{\partial^2 T}{\partial Y^2}\right) \tag{4}$$

Initially the fluid is motionless and isothermal at temperature T_0. The boundary condition is given in Fig 1.

The flow development is determined by three governing parameters: the Rayleigh number (Ra), the Prandtl number (Pr) and the slope (A). They are defined respectively as follows,

$$Ra=\frac{g\beta\Delta T h^3}{\kappa\nu},\quad \Pr=\frac{\nu}{\kappa},\quad A=\frac{h}{l} \tag{5}$$

3. Scaling analysis

First it is proposed a triple layer model for the boundary layer of the natural convection flow, which in particular suits the case $Pr > 1$. A schematic illustration of the boundary layer profile depicting this is shown in Fig. 3. Here, as an important difference from previous scaling analysis, an additional layer, layer II, is introduced, which is normally neglected if the fluid is assumed to be infinitely large Pr-number. An integral approach is used to derive the scaling laws.

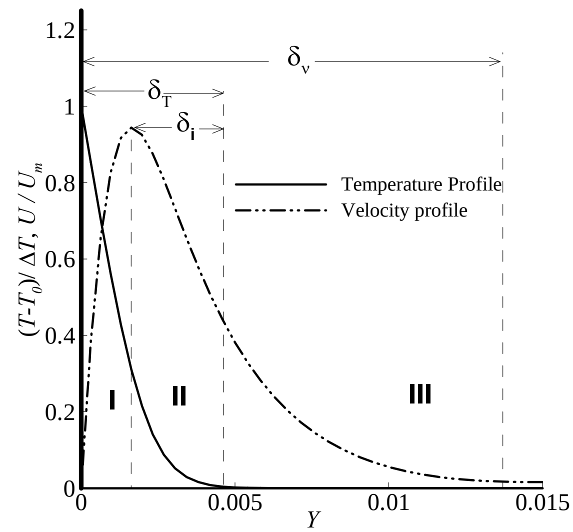

Fig. 2. A schematic of the temperature and velocity profiles normal to the inclined plate at its mid point.

Initially the thermal boundary layer grows according to $\delta_T \sim \kappa^{1/2}t^{1/2}$. In regions I and II, the balance is between viscosity and buoyancy. However, in region III the balance is between viscosity and inertia. In region I (the inner viscous layer), the balance between buoyancy and the viscosity gives:

$$U_m \sim \frac{g\beta\Delta T\sin\phi}{\nu}\left(\delta_T-\delta_i\right)^2 \tag{6}$$

In region II, the limit of the integral is taken between (δ_T-δ_i) and δ_T.

$$0 \sim \nu\left.\frac{\partial U}{\partial Y}\right|_{\delta_T-\delta_i}^{\delta_T}+g\beta\sin\phi\int_{\delta_T-\delta_i}^{\delta_T}TdY \tag{7}$$

Note that $\partial U/\partial Y|_{\delta T-\delta i} = 0$ since the velocity is maximum there. Additionally, we have

$$\left.\frac{\partial U}{\partial Y}\right|_{\delta_T} \sim \frac{U_m}{\delta_\nu-\delta_T+\delta_i} \text{ and } \int_{\delta_T-\delta_i}^{\delta_T}TdY \sim \Delta T\delta_i \tag{8}$$

Hence,

$$U_m \sim \frac{g\beta\Delta T\sin\phi}{\nu}\delta_i\left(\delta_\nu-\delta_T+\delta_i\right) \tag{9}$$

Comparing (6) and (9), we may obtain

$$\delta_i \sim \frac{\delta_T^2}{\delta_T+\delta_\nu} \tag{10}$$

As the buoyancy force is negligible in region III, the flow is driven solely by diffusion of momentum in which the unsteady term balances the viscous term, yielding

$$\frac{U_m}{t} \sim \nu\frac{U_m}{\delta_\nu^2} \tag{11}$$

and further

$$\delta_\nu \sim \nu^{1/2}t^{1/2} \sim \Pr^{1/2}\delta_T \tag{12}$$

Hence, (10) becomes,

$$\delta_i \sim \frac{\kappa^{1/2} t^{1/2}}{1+\Pr^{1/2}} \qquad (13)$$

Additionally, the length of the inner viscous layer (region I) is

$$\delta_T - \delta_i \sim \delta_T - \frac{\delta_T}{1+\Pr^{1/2}} \sim \frac{\Pr^{1/2}}{1+\Pr^{1/2}}\delta_T \sim \frac{\kappa^{1/2} t^{1/2}}{1+\Pr^{-1/2}} \qquad (14)$$

Inserting (13) into (6), we obtain

$$U_m \sim \frac{Ra\kappa^2}{h^3}\frac{A}{\left(1+A^2\right)^{1/2}}\left(\frac{1}{1+\Pr^{-1/2}}\right)^2 t \qquad (15)$$

(15) is the scaling for U_m at the start-up stage

As time increases the more heat is convected away. The boundary layer approaches a steady state until convection balances conduction. Therefore, the steady state scales of time, velocity, thermal layer, inner viscous layer and the total viscous layer are respectively as,

$$t_s \sim \frac{h^2}{Ra^{1/2}\kappa}\frac{\left(1+A^2\right)^{1/2}}{A}\left(1+\Pr^{-1/2}\right) \qquad (16)$$

$$U_{ms} \sim \frac{Ra^{1/2}\kappa}{h}\frac{1}{\left(1+\Pr^{-1/2}\right)} \qquad (17)$$

$$\delta_{Ts} \sim \frac{h}{Ra^{1/4}}\frac{\left(1+A^2\right)^{1/4}}{A^{1/2}}\left(1+\Pr^{-1/2}\right)^{1/2} \qquad (18)$$

$$\delta_{Ts} - \delta_{is} \sim \frac{h}{Ra^{1/4}}\frac{\left(1+A^2\right)^{1/4}}{A^{1/2}}\frac{1}{\left(1+\Pr^{-1/2}\right)^{1/2}} \qquad (19)$$

$$\delta_{vs} \sim \Pr^{1/2}\delta_{Ts} \sim \frac{h}{Ra^{1/4}}\frac{\left(1+A^2\right)^{1/4}}{A^{1/2}}\Pr^{1/2}\left(1+\Pr^{-1/2}\right)^{1/2} \qquad (20)$$

4. Normalization of the governing equations and the scaling

To verify the various scales, numerical solution of the full Navier-stokes equations and energy are obtained for a range of Ra, Pr and A values. For convenience, the non-dimensionalised forms of the governing equations are adopted

$$\frac{\partial u}{\partial x} + \frac{\partial v}{\partial y} = 0 \qquad (21)$$

$$\frac{\partial u}{\partial \tau} + u\frac{\partial u}{\partial x} + v\frac{\partial u}{\partial y} = -\frac{\partial p}{\partial x} + \frac{\Pr}{Ra^{1/2}}\left(\frac{\partial^2 u}{\partial x^2} + \frac{\partial^2 u}{\partial y^2}\right) + \Pr\theta\sin\phi \qquad (22)$$

$$\frac{\partial v}{\partial \tau} + u\frac{\partial v}{\partial x} + v\frac{\partial u}{\partial y} = -\frac{\partial p}{\partial y} + \frac{\Pr}{Ra^{1/2}}\left(\frac{\partial^2 v}{\partial x^2} + \frac{\partial^2 v}{\partial y^2}\right) + \Pr\theta\cos\phi \qquad (23)$$

$$\frac{\partial \theta}{\partial \tau} + u\frac{\partial \theta}{\partial x} + v\frac{\partial \theta}{\partial y} = \frac{1}{Ra^{1/2}}\left(\frac{\partial^2 \theta}{\partial x^2} + \frac{\partial^2 \theta}{\partial y^2}\right) \qquad (24)$$

where x, y, u, v, θ, p and τ are the normalized forms of X, Y, U, V, T, P and t, respectively, which are made normalized by the following set of expressions:

$$x = \frac{X}{h},\quad y = \frac{Y}{h},\quad u = \frac{U}{U_0},\quad v = \frac{V}{U_0},$$
$$\tau = \frac{t}{h/U_0},\quad p = \frac{P}{\rho U_0^2},\quad \theta = \frac{T-T_0}{T_w - T_0} \qquad (25)$$

where $U_0 = \kappa Ra^{1/2}/h$. The origin of the coordinate system is located at the leading edge of the heated plate.

The scaling relations obtained above are normalized as follows:

$$u_m = \frac{U_m}{U_0} \sim \frac{A}{\left(1+A^2\right)^{1/2}}\frac{\tau}{\left(1+\Pr^{-1/2}\right)^2} \qquad (26)$$

$$\tau_s = \frac{t_s}{h/U_0} \sim \frac{\left(1+A^2\right)^{1/2}}{A}\left(1+\Pr^{-1/2}\right) \qquad (27)$$

$$u_{ms} = \frac{U_{ms}}{U_0} \sim \frac{1}{1+\Pr^{-1/2}} \qquad (28)$$

$$\delta_{Ts}^* = \frac{\delta_{Ts}}{h} \sim \frac{\left(1+A^2\right)^{1/4}}{Ra^{1/4}A^{1/2}}\left(1+\Pr^{-1/2}\right)^{1/2} \qquad (29)$$

$$\delta_{Ts}^* - \delta_{is}^* = \frac{\delta_{vis}}{h} \sim \frac{\left(1+A^2\right)^{1/4}}{Ra^{1/4}A^{1/2}}\frac{1}{\left(1+\Pr^{-1/2}\right)^{1/2}} \qquad (30)$$

$$\delta_{vs}^* = \frac{\delta_{vs}}{h} \sim \frac{\left(1+A^2\right)^{1/4}}{Ra^{1/4}A^{1/2}}\Pr^{1/2}\left(1+\Pr^{-1/2}\right)^{1/2} \qquad (31)$$

5. Results and discussions

The velocity and temperature data are taken at x = 0.5, which is sufficiently far from the leading edge and the downstream end of the domain to avoid any end effects. The time series of the maximum velocity parallel to the plate (u_m) has also been recorded on the same line, which has been used to verify the velocity scaling relation.

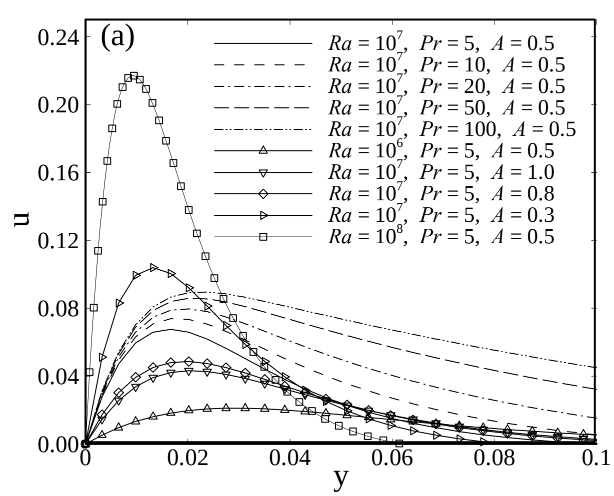

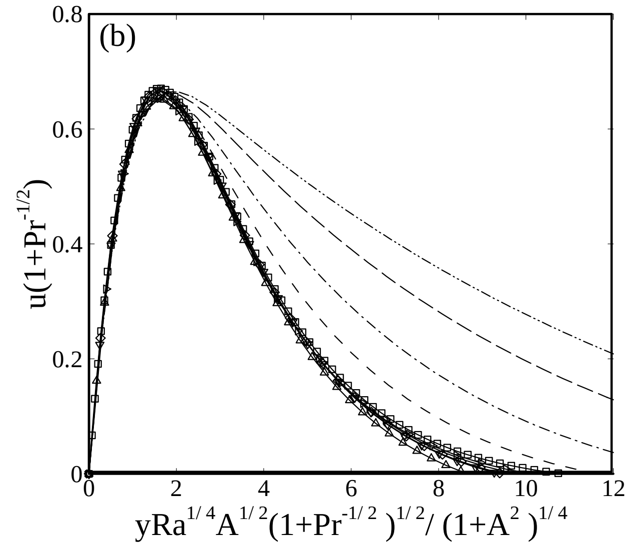

Fig. 3: Velocity profiles parallel to the plate along the line x = 0.5 for all cases considered at steady state: (a) raw data and (b) $u(1+Pr^{-1/2})$ plotted against $yRa^{1/4}A^{1/2}(1+Pr^{-1/2})^{1/2}/(1+A^2)^{1/4}$

The velocity profiles at τ/τ_s = 2.0 (when the flow is fully steady) are shown in Fig. 3 for different Prandtl numbers, Rayleigh numbers and aspect ratios. Fig. 3(a) shows the raw data of the velocity along the line perpendicular to the plate at x = 0.5. In Fig. 3(b), the velocity is normalized by its steady state scale $1/(1+Pr^{-1/2})$ and the distance normalized by its viscous boundary layer thickness scale $(1+A^2)^{1/4}/Ra^{1/4}A^{1/2}(1+Pr^{-1/2})^{1/2}$. Clearly, the scaling relations for the steady state velocity (28) and inner viscous boundary layer thickness (30) agree well with numerical results since all profiles almost overlap onto a single curve in the inner viscous layer (Fig. 3b).

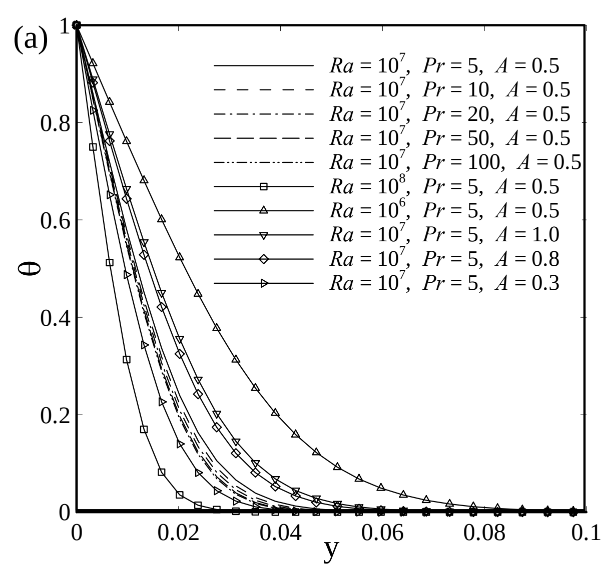

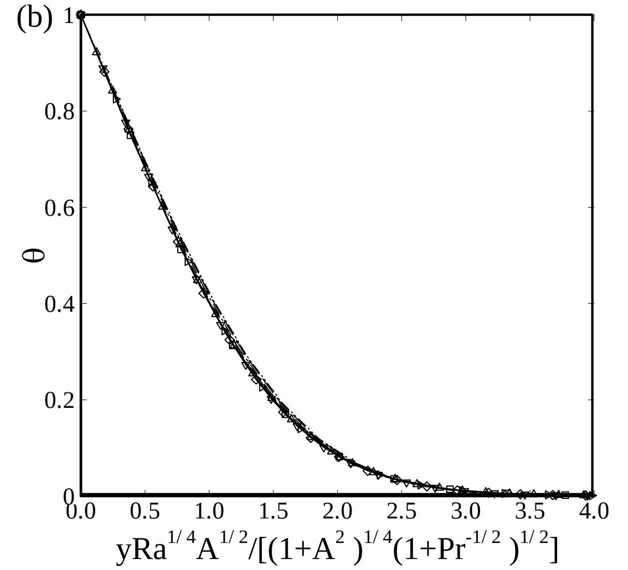

Fig. 4: Temperature profiles along the line x = 0.5 for all cases considered at steady state: (a) raw data and (b) θ plotted against $yRa^{1/4}A^{1/2}/[(1+A^2)^{1/4}(1+Pr^{-1/2})^{1/2}]$

As the boundary-layer development approaches a steady state, the scaling (29) shows that the dimensionless thermal boundary layer thickness, δ_{Ts}, is dependent on Ra, Pr and A. The temperature profiles calculated at x = 0.5 at a steady state are directly presented in Fig. 4(a). The distance y is scaled by $(1+A^2)^{1/4}(1+Pr^{-1/2})^{1/2}/Ra^{1/4}A^{1/2}$ (δ_{Ts} at steady state) and the corresponding temperature profiles are re-plotted in Fig. 4(b). Clearly, all scaled temperature profiles overlap onto a single line, confirming that the scaling (29) is the correct scaling for δ_{Ts} at the steady state.

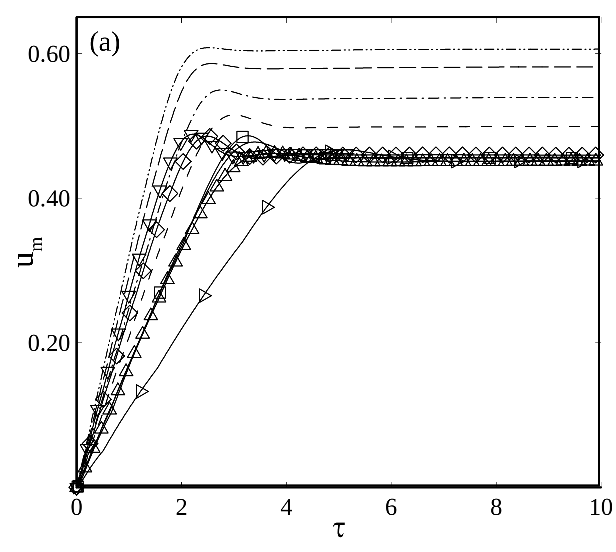

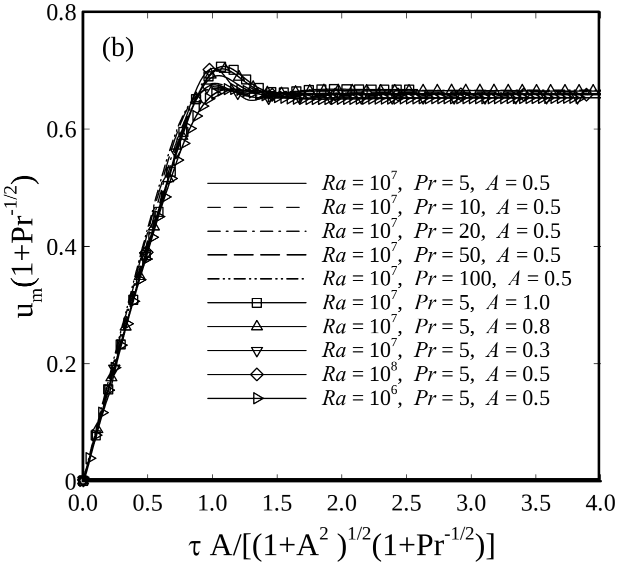

Fig. 5: Time series of the maximum velocity parallel to the plate at x = 0.5 for all cases considered: (a) raw data and (b) $u_m(1+Pr^{-1/2})$ plotted against $\tau A/[(1+A^2)^{1/2}(1+Pr^{-1/2})]$

Fig. 5 presents numerical results to validate the scaling relations (27) and (28). The time series of u_m for varying Ra, Pr and A are presented in figure 5(a). Fig. 5(b) presents the same time series in Fig. 5(a) but with u_m and τ scaled by $1/(1+Pr^{-1/2})$ and $(1+A^2)^{1/2}(1+Pr^{-1/2})/A$, respectively. It is clear that all scaled time series approach the same horizontal straight line at the steady state stage, confirming that $1/(1+Pr^{-1/2})$ is the correct scaling for u_m at the steady state. Additionally, Fig. 5(b) also shows that the peaks of all ten scaled time series occur almost at the same scaled time, validating the scaling relation (27).

6. Conclusions

Natural convection under a heated inclined flat plate is examined by scaling analysis and verified by numerical simulations for various parameters considered here. The verification of the scaling relations includes thermal and viscous boundary-layer developments as well as the heat transfer rate predictions. Numerical results demonstrate that the scaling relations are able to accurately characterize the physical behaviour in each stage of the flow development, including the start-up stage, the transitional stage and the steady state stage. The present scaling analysis incorporates a detailed balance in the momentum equation depending on the thickness of the boundary layer that improves scaling predictions especially where the Pr variation effect is taken into account. The scaling relations are formed based on the established characteristic flow parameters of the maximum velocity in the boundary layer (u_m), the time for the boundary layer to reach the steady state (τ_s) and the thermal (δ_T) and viscous (δ_v) boundary layer thickness. Through comparisons of the scaling relations with the numerical simulations, it is found that the scaling results agree well with the numerical simulations.

References

[1] J. C. Patterson, J. Imberger, Unsteady natural convection in a rectangular cavity, *J. Fluid Mech.* Vol. 100, pp. 65-86, 1980

[2] S.W. Armfield, J.C. Patterson, W. Lin, Scaling investigation of the natural convection boundary layer on an evenly heated plate, *Int. J. Heat Mass Transfer* Vol. 50, pp. 1592–1602, 2007.

[3] W. Lin, S. W. Armfield, Direct simulation of natural convection cooling in a vertical circular cylinder, *Int. J. Heat Mass Transfer*. Vol. 42, pp. 4117–4130, 1999.

[4] W. Lin, S. W. Armfield, Natural convection cooling of rectangular and cylindrical containers, *Int. J. Heat Fluid Flow*. Vol. 22, pp. 72–81, 2001.

[5] W. Lin, S. W. Armfield, Long-term behavior of cooling fluid in a rectangular container, *Phys. Rev. E.* Vol. 69, pp. 05631, 2004.

[6] S. C. Saha, J. C. Patterson, C. Lei, Scaling of natural convection of an inclined flat plate: Sudden cooling condition, *ASME J. Heat Transfer*. (*Accepted*), 2010.

[7] S. C. Saha, J. C. Patterson, C. Lei, Natural convection boundary layer adjacent to an inclined flat plate subject to sudden and ramp heating, *Int. J. Therm. Sci.*. Vol. 49, pp. 1600-1612, 2010.

[8] S. C. Saha, J. C. Patterson, C. Lei, Natural convection in attic-shaped spaces subject to sudden and ramp heating boundary conditions, *Heat and Mass Transfer*. Vol. 46, pp. 621-638, 2010..

[9] S. C. Saha, J. C. Patterson, C. Lei, Natural convection and heat transfer in attics subject to periodic thermal forcing, *Int. J. Therm. Sci.*. Vol. 49, pp. 1899-1910, 2010..

[10] S. C. Saha, J. C. Patterson, C. Lei, Natural convection in attics subject to instantaneous and ramp cooling boundary conditions, *Energy and Buildings*. Vol. 42 pp. 1192-1204, 2010.

[11] D. Poulikakos, A. Bejan, The fluid dynamics of an attic space, *J. Fluid Mech.* Vol. 131, pp. 251–269, 1983.